ASTRONOMY & ASTROPHYSICS
SUPPLEMENT SERIES

Astron. Astrophys. Suppl. Ser. **137**, 233–244 (1999)

UBVI imaging photometry of NGC 6231⋆,⋆⋆

G. Baume, R.A. Vázquez, and A. Feinstein

Observatorio Astronómico de La Plata, Paseo del Bosque s/n, 1900 La Plata and PROFOEG-CONICET, Argentina

Received May 18, 1998; accepted February 4, 1999

Abstract. CCD $UBVI$ photometry in the field of the open cluster NGC 6231 was obtained for 1060 stars down to $V \approx 19$ mag. Memberships, reddening, distance and age of this cluster were investigated. Its lower sequence displays a notorious bend at $V \approx 13.5$ mag followed by a high number of faint stars showing a large magnitude spread at constant colour. This distribution of stars does not seem to be produced by a mere accumulation of field stars seen in the direction of the cluster but by a real star excess in the zone. The evidence suggests these stars are serious candidates to be cluster members caught in their way towards the ZAMS. Fitting them with pre main sequence isochrones an age spread of about 10 Myr is obtained. The luminosity and mass functions were found to be flat for $-7.5 < M_V < 1.5$ and from 3 to 80 $\mathcal{M}_\odot$ respectively.

Key words: cluster: open — individual: NGC 6231 — stars: luminosity function, mass function — HR diagram

1. Introduction

The very young open cluster NGC 6231 ($l = 345.5°$, $b = 1.2°$) is the nucleus of the association Sco OB1 and is responsible of exciting the nebula RCW 113 (Laval 1972) located in the southern part of the association. Its stellar content includes WR-, β Cepheid- and several Of- and O-type stars, many of which show variability and/or have a high chance of being binary systems (Levato & Morrell 1983; Raboud 1996).

This cluster and the overall region of Sco OB1 have been the subject of a comprehensive analysis by Perry et al. (1990, 1991, 1992) from a large compilation of photometric and spectroscopic data. Not much information regarding the cluster lower main sequence structure and the presence of PMS stars can be drawn from this compilation because of its low magnitude limit. Notwithstanding, the authors conclude that all the stars with $V \geq 10$ mag are in a different evolutionary status (pre main sequence stars, PMS) respect of the brightest members. It is timely to recall that in an early investigation of PMS stars, Eggen (1976) suggested that a violent star formation process had taken place there.

Stellar formation seems to be an ongoing process in Sco OB1. Let us mention that magnitude spread at constant colour (currently associated to the presence of PMS stars) was reported in Tr 24, another cluster of this association, by Heske & Wendker (1984, 1985) and that a subgroup of probable PMS stars lying in the field of Sco OB1 was also investigated by Heske & Wendker (1985) and studied in more detail by Piers et al. (1992).

The aim of the present work is to describe the lower cluster structure, looking for PMS evidences, and also to analyse the luminosity and mass distributions of the more massive members. Although broad band photometry does not provide conclusive evidence, on a well established physical ground on the PMS problem, it allows us to inspect the distribution of very faint stars and to look for hints of their presence (e.g. large magnitude spreads at constant colour and star excesses). Firm conclusions on PMS stars need to be supported by, at least, infrared observations and kinematics studies. Two extensive photometric surveys in the area of NGC 6231 have been reported: one by Seggewiss (1968) and another by Raboud et al. (1997). Unfortunately, they are not deep enough to allow a description of the lower main sequence of this cluster, but a new article by Sung et al. (1998) containing $UBVRIH\alpha$ photometry and reporting the detection of PMS stars and PMS candidates here was published. This is an exciting result as, until now, few evidence of stars in contraction towards the ZAMS had been found in open clusters (e.g. Hillenbrand et al. 1993 in NGC 6611).

Send offprint requests to: gbaume@fcaglp.fcaglp.unlp.edu.ar

⋆ Based on observations collected at the University of Toronto Southern Observatory, Las Campanas, Chile.

⋆⋆ Table 1 is available only in electronic form at the CDS via anonymous ftp (130.79.128.5) or via http://cdsweb.u-strasbg.fr/Abstract.html

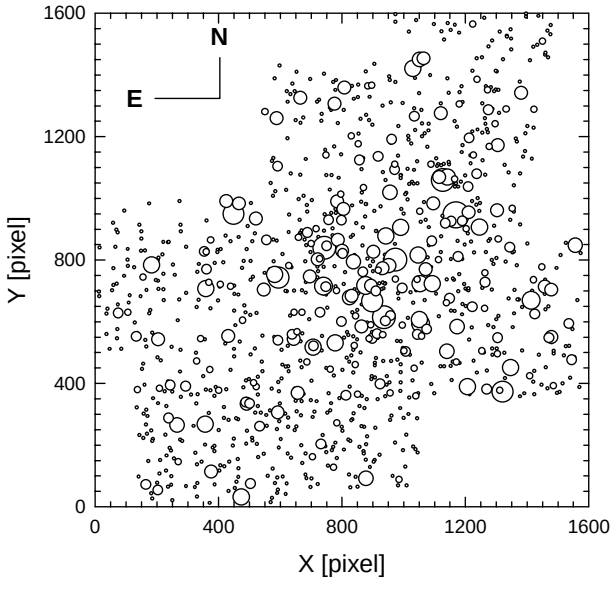

Fig. 1. The finding chart of programme stars in NGC 6231. The size of the symbols is proportional to the star magnitude approximately

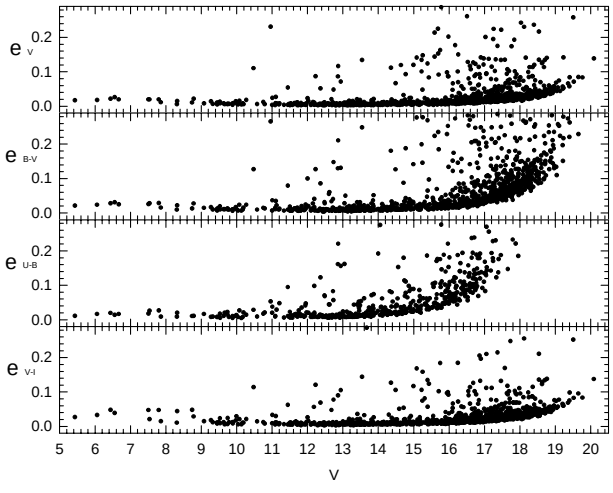

Fig. 2. Photometric errors in magnitude and colour as a function of V magnitude

Since there is a comparable photometric limit between Sung et al.'s (1998) study and ours we will analyse some of their findings in relation to ours.

2. Observations

Figure 1 presents a finding chart of NGC 6231 that shows the eight fields where we obtained $UBVI$ photometry using the 60 cm telescope of the University of Toronto Southern Observatory, Las Campanas, Chile. The observations, that covered an area of 105 squared minutes approximately, were carried out during a 5 day run in May 1995 using a PM 512×512 METHACROME-II, UV coated chip, with a scale of $0.45''$/pixel, covering $4'$ on a side. Typical exposure times per filter were: from 20 to 600 seconds in V, 10 to 1000 in B, 50 to 1800 in U and 10 to 130 in I including mid exposures. As usual, we took two long exposures per filter to improve the statistics of faint stars. Apart from a long exposure frame disturbed by thin clouds that had to be self-calibrated, the entire run was photometric, with mean seeing values ranging from 1.2 to 1.5 arcsec. The complete reduction techniques are described in Vázquez et al. (1996). Instrumental signatures were removed using bias and a combination of dome flats and twilight flats while instrumental magnitudes were produced via point spread function (Stetson 1987).

The observations were tied to the standard $UBVI$ Cousins system using stars in NGC 5606 (Vázquez & Feinstein 1991) and Hogg 16 (Vázquez et al. 1994) systematically measured every night. The residuals left by these "standard" stars (about 30 each night) average less than 0.025 in magnitudes and colours, a value that we adopt as a measure of the external photometric error of the run. An estimate of the internal errors of our photometry was obtained by comparing photometric values of common stars in the overlapping zones among different frames. We found typical mean differences of about 0.025 mag for $V <$ 16 mag in both, colours and magnitudes.

Table 1 contains the final CCD photometry including star numberings, x and y coordinates and magnitudes and colours for 1060 stars. Errors in colours and magnitudes are plotted in Fig. 2 as a function of the V magnitude and a cross-identification of Seggewis (1968) numberings and ours is shown in Table 2.

A comparison of our photometry with Perry et al. (1991, hereafter PHC91), Seggewiss (1968) and Sung et al. (1998, hereafter SBL98) is shown in Table 3. The agreement with these data sets is excellent although we notice large standard deviations respect of the 157 stars in common with Seggewiss, probably because most of his data is photographic what can yield uncertain photometric values among very faint stars.

Several stars showed ΔV differences larger than 3σ respect of PHC91. In some of them the differences could have been produced by star-light contamination of photoelectric measures but in others it would be desirable to carry out further analyses to confirm whether they are real variable stars. All the stars suspected of variability are marked with an (**1**) in Table 1.

To know how much of the cluster we surveyed, we redetermined its size using the Digitized Sky Survey plates (**DSS**). To construct the cluster stellar density profile, star counts were done in concentric rings around a centre previously determined. Then, this profile was fitted using a Gaussian and the cluster limit was set at the point where the stellar density merges into the level background. The procedure gives a 7 arcmins radius and a total area of the cluster of about 150 square minutes so $\approx 70\%$ out of it was observed by us. However, the literature reports two groups

Table 2. Cross-identification with Seggewiss (1968)

#	*Segg.*	#	*Segg.*	#	*Segg.*	#	*Segg.*	#	*Segg.*	#	*Segg.*	#	*Segg.*
1	290	37	261	76	283	122	103	166	235	207	183	260	263
5	220	38	80	77	184	123	219	168	45	208	151	261	156
7	254	39	209	85	142	124	255	169	20	209	228	262	159
8	161	40	294A	91	217	127	234	173	242	211	205	266	154
10	266	41	259	93	278	129	214	175	203	212	134	269	197
11	224	44	213	94	123	130	196	176	85	213	133	274	190
13	292	45	105	95	199	131	273	178	237	216	22	278	244
14	248	47	162	96	284	133	262	180	285	218	231	280	153
16	287	50	16	98	215	136	113	181	88	217	218	282	206
17	286	51	236	100	152	139	276	182	279	220	10	284	201
18	295	52	108	101	230	140	198	183	207	224	229	286	264
19	272	54	186	102	18	141	130	184	141	225	109	287	84
20	253	55	140	103	165	143	122	187	17	227	139	290	149
21	289	56	189	105	243	144	271	189	258	228	157	301	7
22	238	57	194	106	21	146	275	190	239	230	136	303	256
23	150	58	115	109	265	148	225	193	5	231	260	307	135
25	232	66	223	110	227	153	19	196	270	234	188	308	9
26	282	68	137	112	86	155	212	197	81	236	211	310	155
28	110	79	24	113	200	156	252	200	15	241	208	333	226
29	6	70	160	115	43	158	87	201	128	242	116	–	–
30	102	71	222	116	131	160	202	202	241	254	277	–	–
33	34	72	274	117	42	164	23	203	8	257	132	–	–
34	112	73	294B	121	240	165	216	204	129	258	143	–	–

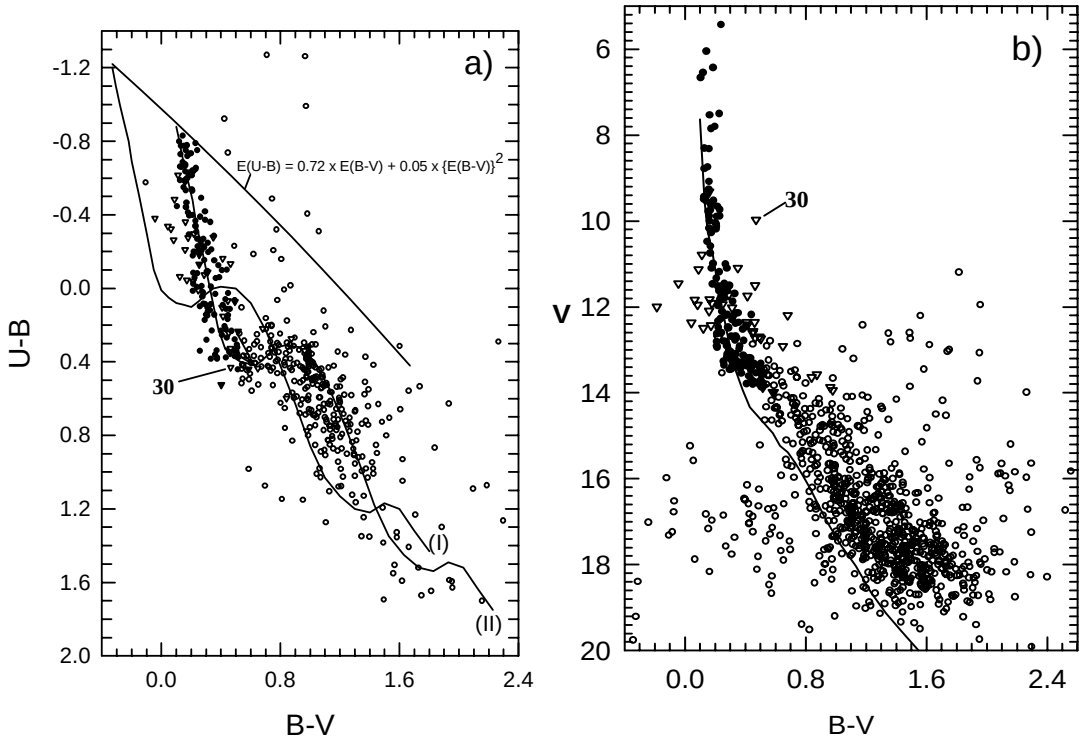

Fig. 3. a) The two-colour diagram of all stars observed in NGC 6231. Filled circles are likely members; filled inverted triangles are probable members; open inverted triangles are non-members. Open circles are stars for which no membership was assessed. Solid lines stand for the intrinsic line for luminosity class V stars, in its normal location (I), and displaced by 0.43 and 0.33 mag in $B-V$ and $U-B$ respectively (II). The path of the reddening is indicated. The location of star # 30 (HD 326338), a non-member δ Scut variable of spectral type F0III and period $P = 0.0896^{\rm d}$ (Balona & Laney 1995) is shown. **b)** The V vs. $B-V$ diagram. Symbols have the same meaning as in **a)**. The solid line is the ZAMS (Schmidt-Kaler 1982) fitted to an apparent distance modulus $V - M_V = 12.90$ and displaced by 0.43 mag in $B-V$

of sizes for NGC 6231: small ones, ≈ 15 arcmins diameter (Shapley 1930; Trumpler 1930), which we favour, and large sizes, ≥ 25 arcmins (Barchatova 1950; Seggewiss 1968). It is worth mentioning that Raboud et al. (1997) (hereafter RCB97) and SBL98 have found members at more than 7 arcmins from the cluster centre what could be interpreted as a mass segregation effect (Raboud & Mermilliod 1998).

3. Data analysis

3.1. Memberships

The determination of memberships in NGC 6231 was carried out inspecting the locations of the stars in all the photometric diagrams simultaneously. From Figs. 3 and 4, the following main features can be outlined:

The two-colour diagram shows, down to $B-V \leq 0.5$ and $U-B \leq 0.4$, a well populated upper main sequence composed by OB- and early A-type stars slightly affected by differential reddening. Since these all stars have unique reddening solution their memberships can be analysed individually. There are also some stars located along the reddening path of OB-type stars that could be heavily reddened background faint stars of early types. But there is no doubt that many others are located there because of large errors in the $U-B$ indices.

The three colour-magnitude diagrams show a broadening of the observed sequence from $V \approx 11$ to $V \approx 13.5$ mag probably produced by contamination of non-member stars of intermediate B-types located slightly in front of or beyond the cluster that could belong to Sco OB1. This broadening ends in a well marked bend at $V \approx 13.5$ mag, longward of which the stars are mostly located in a band that shows the highest density at ≈ 1.5 mag above the ZAMS. That is why the Schmidt-Kaler ZAMS (1982), when fitted to an apparent distance modulus of 12.9 (see Sect. 3.3), does not coincide with the left envelope of the lower sequence.

We will return to this fact in section 4 but, in advance and without denying a sure confusion with non members, if this band is primarily composed of field stars, it draws the attention that no one is found "in the ZAMS" from $V = 14$ to $V = 16$ mag. In view of this, cluster memberships were only determined for stars with $B-V \leq 0.5$ and $V \leq 14$ mag. Stars above these limits were then analysed and given one of the following membership categories: likely members (stars with the highest chances), probable members (stars whose magnitudes and colours are not very well correlated in all the diagrams but with reddening solutions still acceptable) and non-members (obvious cases of inconsistency in all the diagrams). The membership category is listed in Table 1.

3.2. Reddening analysis

To get intrinsic colours we need to know the E_{U-B}/E_{B-V} excess relation valid in the cluster. Table 4 contains a list of the bright stars with CCD photometry whose spectral types were mostly taken from Table 3 of PHC91. This sample was used to determine the reddening curve of NGC 6231. Besides, as the list of PHC91 includes a large number of stars in Sco OB1 having spectral types and UBV photometry, we used this information to perform a more refined analysis of the reddening around the cluster too.

Figure 5 shows the E_{U-B}, E_{B-V} diagram for 43 stars in NGC 6231 taken from Cols. 8 and 9 of Table 4. The same was done for 130 stars in Sco OB1 whose values were not listed for saving space. In both cases, colour excesses were obtained from the Schmidt-Kaler (1982) calibration of intrinsic colours and spectral types. Although most of the stars follow the standard reddening relation $E_{U-B}/E_{B-V} = 0.72 + 0.05 \times E_{B-V}$, it is evident that both excesses are not only widely scattered but also biased towards large values, especially the E_{U-B}. The influence of large E_{U-B} excesses is better understood in Fig. 6 where we see how the distribution of the E_{U-B}/E_{B-V} ratios is biased towards values higher than 0.72. There are two reasons to think this colour excess scatter is intrinsic to the stars themselves and not produced by systematic and/or random errors of our CCD photometry: *a)* our data show high E_{U-B} excesses exactly as PHC91 photoelectric measures of Sco OB1 stars do (both techniques imply different instrumental errors assuming CCD photometry is more accurate) and *b)* PHC91 stellar data are mainly averages of many photometric measures taken from several observers. Therefore, any unusual photometric value of a given star should have been smoothed and no large colour excess scatter should be seen in Fig. 5 among Sco OB1 stars.

The E_{U-B}/E_{B-V} ratios in NGC 6231, listed in Col. 11 of Table 4, show some anomalous values. If, instead of using our CCD data, we consider the Seggewiss (1968) photometry, the anomalies are confirmed in all the cases (except star # 25). Using PHC91 and SBL98 data also yield a similar result. It is interesting that several of these stars are, in addition, binaries or variables, the part of this scatter could be related to this feature as well. Another source of the scatter seen in Figs. 5 and 6 could be related to the interstellar material since Santos & Bica (1993) found that 0.20 mag out of the total reddening affecting NGC 6231 originates in intracluster dust (this would explain the differential reddening seen in the colour-colour diagram too). There is also a nearby molecular cloud in front of Sco OB1 (Dame et al. 1987) while Crawford (1990) reports strong variations in the CN density in the cluster direction.

Averaging the data of Col. 11 in Table 4 it was found $< E_{U-B}/E_{B-V} >= 0.75 \pm 0.19$ (sd) (rejecting stars with

Table 3. Comparison of our photometry with other authors in the sense others minus us

Author	$\langle\Delta V\rangle$	$\langle\Delta(B-V)\rangle$	$\langle\Delta(U-B)\rangle$	$\langle\Delta(V-I)\rangle$	n
PHC91	-0.012 ± 0.045	-0.010 ± 0.036	0.009 ± 0.036		62
Seggewiss	-0.038 ± 0.078	0.037 ± 0.081	0.028 ± 0.078		157
SBL98	0.017 ± 0.052	0.004 ± 0.044	-0.001 ± 0.060	0.028 ± 0.040	153

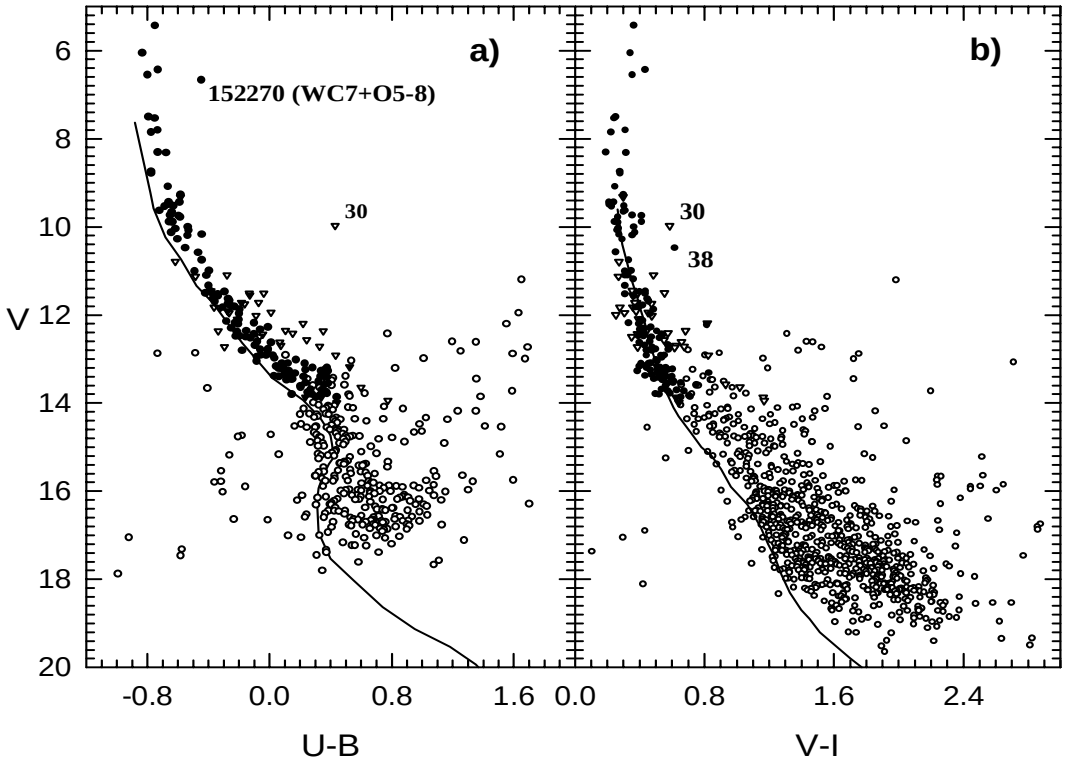

Fig. 4. a) The V vs. $U-B$ diagram. Symbols have the same meaning as in Fig. 3a. The solid line is the ZAMS (Schmidt-Kaler 1982) fitted to an apparent distance modulus $V - M_V = 12.90$ and displaced by 0.33 mag in $V-B$. **b)**. The V vs. $V-I$ diagram. Symbols as in Fig. 3a. Star # 38, (-41°7734) is a probable variable β Ceph for which our CCD measures differ by more than 0.1 in V and $B-V$ in respect of PHC91 values. The ZAMS was derived from Cousins (1978) relation of $B-V$ and $V-I$

very extreme values) while for association stars it was found $< E_{U-B}/E_{B-V} >= 0.75 \pm 0.13$ (excluding 31 stars). These two mean values do not differ from each other significantly neither from the standard slope of 0.72 given above. But, in view of the numerous facts that distort the colour excess ratios, intrinsic colours of likely members without spectral classification were computed through the standard excess relation given above (described in Vázquez et al. 1996). As it is only valid for stars with $B-V \leq 0.5$ and $U-B \leq 0.4$, a few detected probable members (late B- and early A-types) were corrected for average reddenings $< E_{B-V} >= 0.43 \pm 0.04$ and $< E_{U-B} >= 0.33 \pm 0.09$ computed with the data of Table 4.

The R value, A_V/E_{B-V}, that allows to correct visual magnitudes according to $V_0 = V - R \times E_{B-V}$, was estimated from the individual E_{V-I}/E_{B-V} ratios listed in Col. 12 of Table 4. The E_{V-I} excesses were obtained with a calibration of spectral types and $(V-I)_0$ from Cousins (1978). These number ratios average 1.38 ± 0.19 that leads to $R \approx 3.5$, similar to 3.6 derived by Johnson (1968) and not far from 3.3 ± 0.1 found by SBL98. We recall that a number ratio of 1.24 is expected for normal absorbing material having $R = 3.1 - 3.2$ according to Dean et al. (1978). As it is not clear if this large R is due to some of the facts discussed above (including variability and binarity) or to all of them together, we will adopt $R = 3.2$.

To finish this part of the analysis, we re-estimated the absorption $A_V(r)$ in the direction of NGC 6231 using all the stars located within a ring of 25 arcmins radius around it. The photometry and spectroscopy of these stars, outside the area of our survey, were taken from Table 3 of PHC91. Their individual absorption A_V and distances r were computed and plotted in Fig. 7. The structure of $A_V(r)$ seen in this figure is more complex than that shown by Neckel & Klare (1980) constructed with samples of

Table 4. CCD photometry and main characteristics of the brightest stars of NGC 6231

#	*Star desig.*	V	$B-V$	$U-B$	*Spect. Types*	*Rem.*	E_{B-V}	E_{U-B}	E_{V-I}	$\frac{E_{U-B}}{E_{B-V}}$	$\frac{E_{B-V}}{E_{V-I}}$	V_0-M_V
1	152234	5.43	0.24	−0.75	B0.5Ia	B	0.45	0.28	0.58	0.62	1.28	11.89
2	152248	6.06	0.14	−0.83	O7Ib(f)+O6.5f	B, v	0.45	0.32	0.68	0.71	1.51	10.62
3	152249	6.44	0.19	−0.73	OC9.5Iab	B, v	0.44	0.36	0.71	0.82	1.61	11.53
4	152233	6.55	0.12	−0.80	O6III(f)	v	0.44	0.37	0.71	0.84	1.61	11.24
5	152270	6.67	0.10	−0.45	WC7+O5-8	B						
6	326331	7.51	0.23	−0.79	O7.5IIIF	B? v	0.54	0.34	0.60	0.63	1.11	11.58
7	152219	7.54	0.16	−0.75	O9.5III	B, v	0.46	0.35	0.57	0.76	1.23	11.36
8	152314	7.80	0.20	−0.73	O9.5III-IV	B, v	0.50	0.37	0.64	0.74	1.28	11.50
9	−41°7733	7.86	0.17	−0.78	O9III	B, v	0.48	0.34	0.57	0.71	1.18	11.92
10	152200	8.31	0.13	−0.73	O9.5III	B, v	0.43	0.37	0.52	0.86	1.20	12.23
11	−41°7742	8.32	0.16	−0.67	O9IV	B, v	0.47	0.45	0.66	0.96	1.40	12.01
13	326329	8.78	0.13	−0.77	O9V	v^1	0.44	0.35	0.62	0.79	1.40	11.87
14	−41°7712	9.08	0.16	−0.67	B0IV		0.46	0.41	0.58	0.89	1.26	12.30
16	−41°7730	9.32	0.16	−0.58	B1V		0.42	0.37	0.59	0.88	1.40	11.17
17	−41°7727	9.45	0.13	−0.59	B1V	*	0.39	0.36	0.53	0.92	1.35	11.40
18	−41°7723	9.45	0.13	−0.66	B1V	B	0.39	0.29	0.50	0.74	1.28	11.40
20	−41°7706	9.53	0.19	−0.63	B1V+B1V	B, βCeph	0.45	0.32	0.59	0.71	1.31	11.29
21	−41°7724	9.54	0.14	−0.69	B0.5V	B, βCeph?	0.42	0.32	0.53	0.76	1.26	11.79
22	326330	9.64	0.16	−0.65	B0.5V	βCeph	0.44	0.36	0.61	0.81	1.38	11.83
23	326333	9.66	0.21	−0.64	B1V	βCeph	0.47	0.31	0.59	0.65	1.25	11.35
24	326332	9.74	0.23	−0.65	B0.5V		0.51	0.36	0.65	0.70	1.27	11.70
25	−41°7743	9.75	0.17	−0.59	B0.5V	B, v	0.45	0.42	0.71	0.93	1.57	11.91
26	−41°7711	9.78	0.15	−0.58	B2V+B2V	βCeph	0.39	0.26	0.53	0.66	1.35	10.93
28	−41°7753	9.89	0.23	−0.66	B1V	βCeph	0.49	0.29	0.70	0.59	1.42	11.52
29	−41°7725	9.90	0.21	−0.64	B0V		0.51	0.44	0.60	0.86	1.17	12.26
32	−41°7722	10.04	0.20	−0.61	B1V		0.46	0.34	0.56	0.73	1.21	11.76
33	326328	10.08	0.21	-0.53	B1.5V		0.46	0.30	0.58	0.65	1.26	11.30
34	−41°7755	10.13	0.21	−0.64	B1V		0.47	0.31	0.66	0.65	1.40	11.82
36	−41°7736	10.19	0.21	−0.54	B1V		0.47	0.41	0.64	0.87	1.36	11.88
37	−41°7715	10.28	0.17	−0.60	B2IV-V	βCeph,*	0.41	0.24	0.55	0.58	1.34	12.06
38	−41°7734	10.48	0.15	−0.55	B0V	βCeph?, v^1	0.45	0.53	0.95	1.17	2.11	13.04
39	Ho86	10.58	0.17	−0.47	B2IV-V	*	0.41	0.37	0.51	0.90	1.24	12.36
40	−41°7737	10.76	0.17	−0.44	B1.5V		0.42	0.46	0.60	1.09	1.42	12.11
41	Ho84	10.79	0.11	−0.62	B3(V)	v^1	0.31	0.09	0.47	0.29	1.51	11.39
44	Seg 213	11.01	0.27	−0.49	B2IV		0.51	0.35	0.57	0.68	1.11	12.47
66	Seg 223	11.72	0.25	−0.18	B6V		0.40	0.32	0.52	0.80	1.30	11.34
71	Seg 222	11.81	0.24	−0.23	B4V		0.42	0.41	0.58	0.97	1.38	11.86
72	Seg 274	11.82	0.16	−0.36	B3V	v^1	0.36	0.35	0.56	0.97	1.55	12.26
91	Seg 217	12.21	0.27	−0.21	B6V		0.42	0.29	0.54	0.69	1.28	11.76
110	Seg 227	12.50	0.29	−0.15	B7V	*	0.42	0.28	0.59	0.66	1.40	11.75
127	Seg 234	12.78	0.33	−0.01	B8V		0.44	0.33	0.60	0.75	1.36	11.62
131	Seg 273	12.81	0.21	−0.18	B9IV	*	0.28	0.02	0.51	0.07	1.82	12.11
148	Seg 225	13.06	0.30	−0.08	B9V	v^1	0.37	0.12	0.57	0.32	1.54	11.76
166	Seg 235	13.27	0.33	–	B8.5V	v? v^1	0.42	0.27	–	0.64	–	11.92

Note: Details of membership can be found in Table 1. "Seg" is for Seggewiss (1968) and "Ho" is for Houck (1956) numberings respectively. The main source of spectral types has been the PHC91 article and Levato & Morrell (1983). V_0-M_V column contains spectrophotometric moduli.

Remarks: v^1 probable variable according to the ΔV differences with PHC91 photometry. See also Table 1.
v = variable; v? = variable?
B = binary (from PHC91)
$*$ = binary according to Raboud (1996).

OB-type stars. As OB stars are commonly far from the Sun, their sampling does not inform much about local variations of the absorption. After making some attempts, we found that $A_V(r)$ is better described by:

$$A_V(r) = \begin{cases} -1.65 + 0.93\times\log(r), & 0.05 \text{ Kpc} < r < 1.8 \text{ Kpc} \\ 1.4 & 1.8 < r < 2.7 \text{ Kpc} \\ 0.00123 \times r - 1.92 & 2.7 < r < 4 \text{ Kpc} \\ 3 & r > 4 \text{ Kpc.} \end{cases}$$

for r in parsecs. Within the small volume of the cluster the second value of the array remains the same from 1.8 to 2.7 Kpc in agreement with PHC91. The third value was obtained making a straight fit from 2.7 Kpc to 4 Kpc whereupon we adopted the extinction curve proposed by Seggewiss (1968).

Figure 7 confirms thus, that most of the absorption in the direction of NGC 6231 takes place in the solar neighbourhood as stated by van Genderen et al.

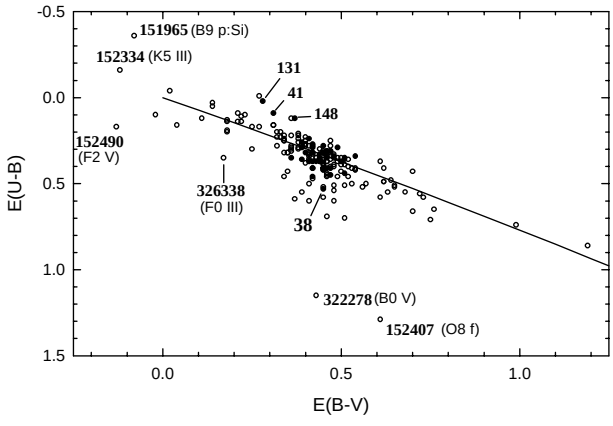

Fig. 5. The E_{U-B} vs. E_{B-V} diagram. Open and filled circles stand for stars in the field of the Sco OB1 and member stars of NGC 6231 respectively. The line is the normal E_{U-B}/E_{B-V} excess relation. Some foreground stars show very anomalous excess relations. Stars # 41 and 148 are probable variables. # 38 is a probable β Ceph and # 131 is a binary according to Raboud (1996)

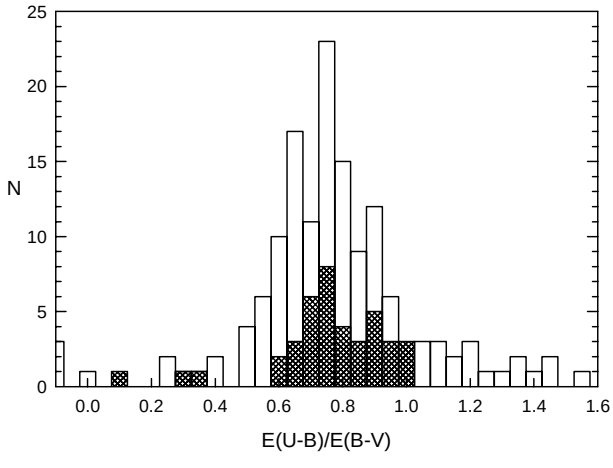

Fig. 6. The E_{U_B}/E_{B-V} distributions for Sco OB1 stars (clean histogram) and cluster stars (hatched histogram)

(1984) and PHC91. RCB97 have also arrived to the same conclusion by investigating the absorption within fields extending $\pm 10°$ and $\pm 2°$ relative to the cluster finding, in addition, that some matter is present at the cluster distance. Like in the earlier works of Shobbrook (1983), Massa & Fitzpatrick (1986) and Balona & Laney (1995), the area covered in our survey is small enough to notice a variation of the reddening across the cluster surface. However, as RCB97 demonstrated (confirmed latterly by SBL98), that is the reddening across NGC 6231 is variable and increases towards its southern part.

3.3. The cluster distance and age

Regarding the cluster distance modulus of NGC 6231 the literature reports values ranging from 10.2 (Kholopov 1980) to 11.6 (Garrison & Schild 1979).

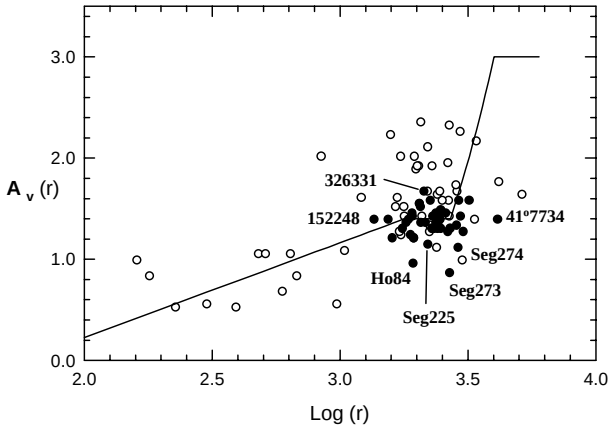

Fig. 7. The line is the path of $A_V(r)$ in the direction to NGC 6231. Open circles are stars located within a circle of 25 arcmin radius around NGC 6231 which data are from PHC91; filled circles are likely cluster members. Stars with peculiar distance modulus are indicated (see details in Table 4)

Individual distance moduli listed in Col. 13 of Table 4 were obtained here from a calibration of spectral types and M_V (Schmidt-Kaler 1982). They average 11.7 ± 0.4 (sd). This high standard deviation is likely to be produced by factors such as the intrinsic scatter among the $M_V s$ of early type stars (Conti 1988) and the numerous known binaries and variables populating the upper main sequence of this cluster.

Another distance estimate, not much affected by binarity, stems from fitting the Schmidt-Kaler (1982) ZAMS in both, the V_0 vs. $(B-V)_0$ and V_0 vs. $(U-B)_0$ diagrams constructed only with likely members. This fitting yields $V_0 - M_V = 11.45 \pm 0.2$ (error from inspection) but we adopted a final value of $V_0 - M_V = 11.5 \pm 0.25$ corresponding to a distance $d = 1990 \pm 200$ pc. The fitting of the ZAMS is shown in the M_V vs. $(B-V)_0$ diagram of Fig. 8, along with the envelope of binaries 0.75 mag above it. Curiously some likely members remain above this envelope as if they were binaries but two of them, # 93 (Segg 278) and 95 (Segg 199), were also investigated by Raboud (1996) who did not find any evidence of binarity.

PHC91 found a distance modulus of 11.50 that agrees with ours, but SBL98 found 11.0 while Balona & Laney (1995) and van Genderen et al. 1984 found 11.08 and 11.0 respectively. In the last two cases, part of the disagreement originates in the use of distinct ZAMSs (they used the Balona & Shobbrook's 1984), but also because they attempted to fit the faint stars which are clearly located above the ZAMS. If we had tried the same procedure here, we would have obtained a distance modulus reduced by 0.6 mag. In turn, SBL98 obtained 11.0 using the ZAMS of Mermilliod (1981) which being hotter than the Schmidt-Kaler's (1982) yields thus smaller distances.

To estimate the age of NGC 6231 we used the isochrones from evolutionary models computed by

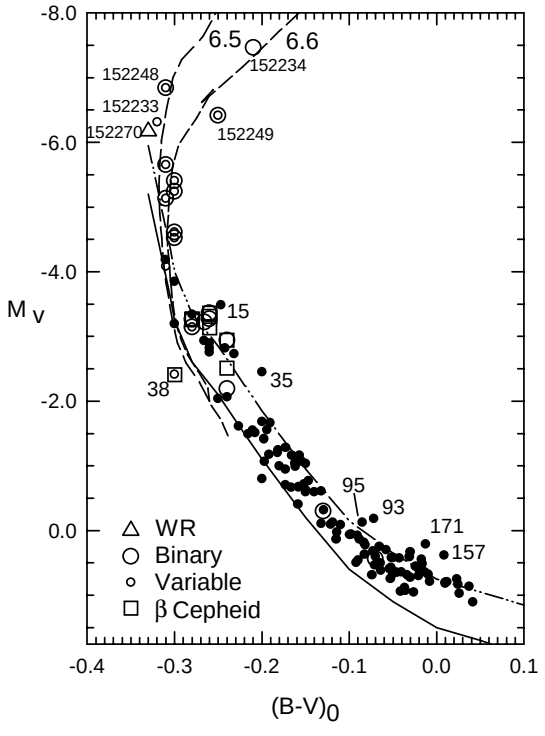

Fig. 8. The M_V vs. $(B-V)_0$ diagram of the brightest stars in NGC 6231. The solid line is the Schmidt-Kaler (1982) ZAMS fitted to $V_0 - M_V = 11.5$; the binary envelope, 0.75 mag above the ZAMS, is the dotted-dashed line and the isochrones of $\log(\tau) = 6.6$ and 6.5 from Schaller et al. (1992) are shown with dashed lines. HD numbers and our star designation are indicated along with the meaning of the symbols. Filled circles are for stars without known peculiarity

Schaller et al. (1992) including mass loss and overshooting and solar metallicity. We assumed that solar metallicity models are applicable in this case although Kilian et al. (1994) indicate that the metallicity of NGC 6231 is lower than solar (but higher than in other clusters). Except the star HD 152233, a single variable star, all the stars with $M_V \leq -4.5$ are binaries. Above this magnitude the sequence is vertical, so by removing binarity, the only appreciable effect is a decrease in the magnitudes of the evolved stars HD 152234 and 152249 that leads to a larger age of the cluster. Given the combined effects of binarity and variability, is not simple to find the best isochrone fitting but if we neglect the even more uncertain location of the WR star HD 152270, the age of the cluster is between 3 and 5 10^6 yr. This range of age is in close agreement with the cluster age given by Santos & Bica (1993), RCB97 and SBL98.

NGC 6231 contains several β Ceph indicated in Fig. 8 and Table 4 which are located 1 mag below the cluster turn-off ($\approx M_V = -4$). The discussion of these stars is out of the scope of our work but in principle there is no conflict with the cluster age and the location in the sequence of these stars as it has been already accepted that they are not necessarily at the end of the core hydrogen burning phase and can display the β Cepheid feature even before reaching that phase (Balona & Shobbrook 1983; Jerzykiewicz et al. 1996).

4. The colour-magnitude diagram of NGC 6231

We have said above that the most noticeable feature of the colour-magnitude diagram is the bend at $V \approx 13.5$ mag followed by a star band 2 mag broad located 1.5 mag above the ZAMS, approximately. For us, the ZAMS sector for $14 < V < 16$ mag with almost no stars on it cannot be explained by anomalies in the $B-V$ indices since the V, $V-I$ diagram shows a similar picture. The respective diagrams of SBL98 and, less notoriously, those of Seggewiss (1968), Balona & Laney (1995) and RCB97 confirm this feature.

A rough way to prove whether such a distribution of faint stars is intrinsic to NGC 6231, is to compute the number of field stars expected in this diagram and subtract them from our observations. Cluster stars together with field stars of a variety of absolute magnitudes, different colour indices, located all at different distances and distinctly reddened, are expected to be included in our photometry. Making an arbitrary subdivision of the observed colour-magnitude diagram, say into cells of size $\Delta V = 1.0$ and $\Delta(B-V) = 0.25$, the removal of expected field stars can be easily performed.

The contribution of field stars within each cell was estimated adding the stars distributed in layers of thickness Δr at distance r within the solid angle dω, subtended by the effective cluster area covered by our survey, using the function:

$$\psi(M_V, ST, r, \Delta r) = \Psi(M_V, ST)\Delta r \mathrm{d}\omega r^2.$$

where $\Psi(M_V, ST)$ is the number of stars per cubic parsec of magnitude absolute M_V and spectral type ST as currently tabulated (see Scalo 1986). As faint cluster stars do not have spectral types but only colour indices and apparent magnitudes, the function $\Psi(M_V, ST)$ had to be transformed adopting $V = M_V - 5 + 5\log r + A_V(r)$, $A_V(r) = 3.2 \times E_{B-V}$ and the relation of spectral types and intrinsic colour indices. Stars of all luminosity classes were considered in the calculation. $A_V(r)$ was taken from Sect. 3.2. It was also assumed that the function $\Psi(M_V, ST)$ should not change significantly along the plane of the Galaxy and would remain valid over large distances (Mihalas 1967). The total contribution of field stars was estimated integrating in layers of $\Delta r = 100$ pc up to a distance of 5 Kpc.

Figure 9 shows, in the form of a contour map, the result of subtracting the expected stars in each cell. The map confirms the existence of a 2 magnitudes broad band rising above the ZAMS at $V \approx 14$ including a density peak at $16.5 < V < 17.5$ and $1.0 < B-V < 1.5$. In any case, the excess of stars that are defining the level curves is larger

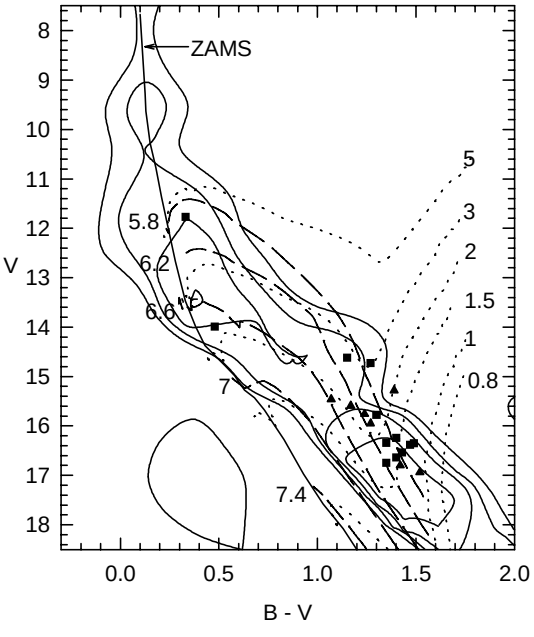

Fig. 9. The contour map of the zone of NGC 6231 after the subtraction of field stars. Solid lines are the density constant loci for 3, 10, 20 and 30 stars. Dotted lines are the PMS evolutionary tracks from Bernasconi & Maeder (1996). The isochrones are indicated with dashed lines and the ZAMS (Schmidt-Kaler 1982) is also shown. Squares and triangles are PMS stars and PMS candidates from SBL98

than the uncertainty of the counts, assuming the uncertainty in a count N is $\sqrt{N}$. Longward of $V \approx 16$ mag, along the ZAMS, the expected numbers of stars largely surpass the observed ones producing negative counts (not shown in the map) while to the right side of the band, there is no difference between the expected and observed numbers of stars. In a simple way, Fig. 9 provides a rough evidence of an excess of faint stars in NGC 6231; but it is not indicating by itself that the stars lying in the band are all cluster members. Indeed, many of them are likely to be of types A, F and G surely related to the cluster, while others may be reddened field stars, even of type B.

A dozen of PMS stars and seven PMS candidates were found by SBL98 in this cluster using a criterion based in Hα emission. Our survey includes none of their PMS candidates and only 7 out of 12 of their PMS stars. Whereas these 7 stars are all well located in the red extreme of our band, it seems that more PMS should have been detected by SBL98 between $0.5 \leq B-V \leq 1.2$. They had already noticed this deficiency arguing that their criterion, based on Hα emission, does not work in all the cases, especially when the material surrounding some PMS stars could have been swept away by stellar winds from massive stars or some supernova event. These authors justified this assumption by a hole seen in the reddening material near the centre of NGC 6231. Whatever the reason in the failure to detect PMS stars, it seems that the UBV photometry can still provide indirect evidences of their presence here.

More information can come from this PMS zone if we superimpose in Fig. 9 the PMS evolutionary models developed under canonical assumptions by Bernasconi & Maeder (1996) and the isochrones derived from them. Here we see how the PMS star region is enclosed by the isochrones of 6 10^5 and 10^7 yr approximately, and masses from $3-5$ $\mathcal{M}_\odot$ for the most massive PMS star to about 1 $\mathcal{M}_\odot$ for the less massive ones are observed. This suggests the existence of an age scatter of 10^7 yr among faint stars which confirms the results from SBL98. All this acts against coevality as the evidences favour that massive and less massive stars formed in different events, the most massive ones being the youngest generation.

4.1. The cluster luminosity function

The luminosity function, LF, is defined as:

$$\mathrm{d}\log(n(M_V))/\mathrm{d}M_V = \gamma \times M_V$$

where $\mathrm{d}\log(n(M_V))/\mathrm{d}M_V$ is the $\log_{10}$ of the number of stars having absolute magnitudes $M_V \pm \mathrm{d}M_V/2$.

Let us briefly comment some factors that may influence the LF reliability:

1.- Data completeness: this is usually the most important one, but according to the M_V range of likely members, the LF will be computed within the range $-7.5 < M_V < 1.5$ mag where we are immune to it.

2.- Binarity or stellar duplicity: these effects that produce a less steep slope remain still unknown factors in NGC 6231 although estimates from Levato & Morrell (1983) and Raboud (1996) indicate minimum binarity percentages of 41% and 52% respectively. Trying to reduce the influence of known binaries we corrected by $\Delta M_V = 0.75$ mag when both components have similar spectral types and 0.50 mag when no information other than binarity was available.

3.- Photometric errors: they normally act raising the magnitude distribution giving thus a steep slope. Their influence on the present case is a negligible effect of less than 1%, even assuming variable errors (magnitude dependent) like those shown in Fig. 2.

Since we know from previous sections that stars with $V \geq 13.5$ mag might be in a different evolutionary status, where the hydrogen burning phase has not started yet, they were not considered for computing the LF. But the evolved members were all included, in principle, because their stage of evolution is not so advanced to exclude them.

The stars were distributed into bins of $\Delta M_V = 1$ mag (using $\Delta M_V = 0.5$ does not modify the result at all) as indicated in Table 5. The WR-type star, HD 152270, the most evolved cluster member, was included in the highest ΔM_V bin.

Three cases were chosen to assess γ. In first term, we used the entire range of M_V, this is $-7.5 < M_V < 1.5$. Next, we excluded the first three bins that contain evolved

Table 5. The luminosity and mass functions of NGC 6231

The luminosity function				
	binarity correction		no binarity correction	
ΔM_V	$< M_V >$	N	$< M_V >$	N
−7.5, −6.5	−7.00	2	−7.15	3
−6.5, −5.5	−6.14	3	−6.12	3
−5.5, −4.5	−4.86	4	−4.98	5
−4.5, −3.5	−4.04	5	−4.04	3
−3.5, −2.5	−2.99	20	−3.10	21
−2.5, −1.5	−1.91	12	−1.88	11
−1.5, −0.5	−0.96	26	−0.96	26
−0.5, 0.5	0.15	32	0.15	32
0.5, 1.5	0.72	33	0.72	33
$Case1$	$\gamma = 0.16 \pm 0.02$		$\gamma = 0.15 \pm 0.02$	
$Case2$	$\gamma = 0.13 \pm 0.04$		$\gamma = 0.13 \pm 0.06$	
$Case3$	$\gamma = 0.14 \pm 0.06$		$\gamma = 0.15 \pm 0.08$	
The initial mass function				
	binarity correction		no binarity correction	
$\Delta\mathcal{M}$	$\log\langle\mathcal{M}\rangle$	$\log N$	$\log\langle\mathcal{M}\rangle$	$\log N$
$128 - 64$	1.82	0.30	1.86	0.47
$64 - 32$	1.58	0.60	1.61	0.47
$32 - 16$	1.30	0.95	1.36	0.90
$16 - 8$	1.05	1.38	1.06	1.39
$8 - 4$	0.74	1.53	0.74	1.53
$4 - 2$	0.44	1.80	0.44	1.80
	$x = 1.14 \pm 0.10$		$x = 1.06 \pm 0.17$	

Note 1: Case 1, the entire ΔM_V range is used to the fitting. Case 2, the first three brightest bins are excluded. Case 3, as in Case 2 but excluding the last bin too. **Note 2**: the lowest mass bin was not used to compute the IMF.

stars. And finally, we ignore, in addition, the lowest M_V bin which is supposed to be affected of incompleteness due to our arbitrary choice of colour and magnitude limits up to which memberships were estimated.

A weighted fit of the data in Table 5 gives slope values of the LF which in no case are larger than 0.20 (assuming uncertainties in each luminosity bin proportional to $\sqrt{N}$). These values disagree with Perry & Hill (1992) who found $\gamma = 0.32$, a discrepancy that could hardly stem from a different fitting procedure despite they made an unweighted fitting (without quoting the slope error). Probably, this discrepancy has an explanation in the fact that Perry & Hill obtained a LF mixing stars of NGC 6231 and stars of Sco OB1. Raboud (1998) covered an area larger than ours but smaller than that of Perry & Hill, obtaining also a flat slope of the LF in this cluster.

4.2. The initial mass function

The term "initial mass function", IMF, is not strictly applicable in this cluster since it requires that all stars were formed at a same time in a same point. As it was said above, the presence of probable contracting stars gives hints against coevality. But if we only consider the likely and probable members, the cluster mass spectrum could still be seen as the cluster initial mass function. On this ground, the slope of the IMF is defined as:

$$x = \log(\mathrm{d}N/\Delta \log \mathcal{M})/\log(\mathcal{M})$$

where the IMF is assumed to be a power law.

Individual stellar masses of members were computed through an interpolation procedure among evolutionary tracks computed with mass loss and overshooting (Schaller et al. 1992). M_V, $(B-V)_0$ and $(U-B)_0$ values were converted to $\log(L/L_0)$ and $\log T_{\rm eff}$ via a relation between effective temperatures, spectral types, colour indices and bolometric corrections given by Schmidt-Kaler (1982). In this plane, the stellar path from the point a star evolved off the ZAMS was reconstructed with the theoretical parameters of the two adjacent evolutionary tracks and the initial mass was then obtained. The WR star (HD 152270) was given a mass similar to the highest stellar mass found in NGC 6231 as we assumed it has evolved the first. Like in the precedent subsection and before computing their masses, binaries were treated introducing ΔM_V corrections already explained.

Stellar masses were included into the mass range indicated in Table 5 and a weighted fit was then made (uncertainties in each mass bins proportional to $\sqrt{N}$). Two values of x, depending on whether binarity is taken into account or not, are shown at the bottom of the same table and the corresponding data fits are shown in Fig. 10.

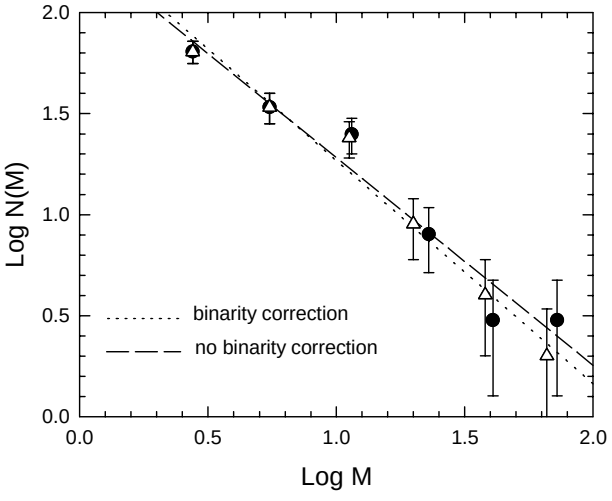

Fig. 10. The Initial Mass Function of likely members in NGC 6231. Dotted line and open triangles represent the case of binarity correction. Long dashed line and filled circles are for no correction

Evidently, binary corrections introduce no appreciable differences in the resulting slopes (1.14 or 1.06) and, according to the errors, at 2σ level, they still approximate the Salpeters (1955) law slope.

SBL98 determined the cluster IMF finding a slope of 1.2 ± 0.4 and a turnover at $\log \mathcal{M} = 0.4$. We found a similar turnover chiefly stated by means of an arbitrary choice of membership and the presence of the bend in the colour-magnitude diagrams instead of the decrease in the number of low mass stars as SBL98 did. For this reason the last mass bin of Table 5 was not used to compute the IMF but it is gratifying the coincidence with SBL98s turnover. They also mention a probable flattening of the IMF for $\log \mathcal{M} \geq 1.2$ which is weakly evident too in Fig. 10 for $\log \mathcal{M} \geq 1.4$ when no binarity correction is adopted. But the same figure shows that this effect, disappears immediately after such correction is done.

SBL98 did not correct their data for binarity and found a IMF slope of 1.21. In our case of no binarity correction, we found a slope of 1.06. It would be easy to assume this difference is produced by a different statistical treatment, but no more than half of it could be explained this way. It seems more realistic to resort to a primordial radial mass segregation effect (Raboud & Mermilliod 1998) where the less massive stars tend to lie outside the cluster centre. In this case, the slope of the mass function is strongly dependent of the area under analysis and the photometric limit. Our area of observation is ≈ 100 square minutes while the field analyzed by SBL98 is ≈ 400 square minutes. Within our area the number of stars with $\log \mathcal{M} \geq 0.4$ used to compute the IMF is ≈ 121 out of 136 stars while SBL98 used ≈ 190 out of 204 stars. Most of the ≈ 70 stars in excess contained in the sample of SBL98 are less massive stars what supports the idea of radial mass segregation.

5. Conclusions

We have investigated NGC 6231 with broad band photometry finding that this cluster is located at a distance of $d = 1990$ pc. The absorption in the direction of NGC 6231 is quite normal although it is seen through nearby molecular clouds. The differential reddening and the large colour excess scatter may be due to a combination of factors such as anomalies of the intracluster material, and also to the presence of several binaries and variables. An isochrone fitting to the upper main sequence stars gives a nuclear age of $3 - 5$ Myr for this cluster.

NGC 6231 shows a bend at $V \approx 13.5$ mag followed by a scarcity of ZAMS stars for $14 < V < 16$. Besides, faint stars here exhibit the peculiarity of being all above the ZAMS without following its shape. Shobbrook (1983) stated that *"... significant number of type A pre-main sequence stars might be found here in a search amongst still fainter members..."*. We attempted to know how many of the observed faint stars are field stars seen against the cluster surface integrating the function $\psi(M_V, ST, r, \Delta r)$ over the distance.

We are aware that the use of a local luminosity function might weaken our argument but, thinking as Underhill (1960) did, it should be proven first that $\Psi(M_V, ST)$ is anomalous in this particular direction. We consider, however, that to know exactly the field star luminosity function here, a deep photometric survey around NGC 6231 should be performed. Once the number of field stars was removed from our star sample a contour map with the star excess was built. This map clearly defines a zone of PMS stars in our HR diagram where, in addition, the PMS stars found by SBL98 are perfectly placed in.

The PMS zone found in NGC 6231 suggests an age spread of about 10 Myr, incompatible with the age derived from bright (massive) members. That is, the less massive stars formed in a timescale of 10 Myr whereas the most massive stars formed in the last $3-5$ Myr, which is against a coeval process.

Concerning the IMF slope, this is the fourth very young open cluster included in our series which slope is flatter than the one given by Salpeter (1955). We have previously found $x = 1.1$ in Tr 14, 1.04 in Pismis 20, 1.09 in NGC 5606 (Vázquez et al. 1996, 1995, 1994, respectively). A preliminary analysis of another galactic cluster in our series, NGC 3293 (Baume et al. 1999), yields that $x = 1.15$, similar to the young LMC cluster NGC 1962-65-66-70 (Will et al. 1995) with $x = 1.0$ to 1.2 or Cyg OB2, another galactic young region with $x = 1.0$ (Massey & Thompson 1991). Notwithstanding the slopes of galactic and magellanic young clusters average $x = 1.3$ (see the compilation of Will 1996) it appears that the "extremely" young ones (ages $< 10^7$ yr) show flatter slopes than the field stars.

Flat slopes, however, could be produced by overestimating the masses of very hot stars or by a mass segregation effect as suggested by RCB97 for NGC 6231. Concerning the first case, up to now there is no conclusive way to know the masses of very hot stars (except for a few cases), as they are mainly obtained from the theoretical HR diagram. A way to reduce the impact of our ignorance of stellar masses is using the procedure of Burki (1977) who detected clusters having abnormal high number of massive stars through a comparative analysis of their respective LFs. In relation to the mass segregation effect, more extensive surveys are necessary, searching for coronal members in several young open clusters.

This article is partially based in the **Digitized Sky Survey** *that was produced at the Space Telescope Science Institute under US government grant NAG W-2166. Original plate material is copyright the Royal Observatory Edinburgh and the Anglo-Australian Observatory.*

Acknowledgements. The authors are indebted to Dr. Garrison for the allocation of telescope time. G. Baume made this work while a grant from the CONICET. We want to thank the useful comments made by Dr. Raboud to improve this manuscript.

References

Balona L.A., Shobbrook R.R., 1983, MNRAS 205, 309
Balona L.A., Shobbrook R.R., 1984, MNRAS 211, 375
Balona L.A., Laney C.D., 1995, MNRAS 276, 627
Barchatova K.A., 1950, Russ. AJ 27, 180
Baume G., Vázquez R.A., Feinstein A., 1999 (to be submitted)
Bernasconi P.A., Maeder A., 1996, A&A 307, 829
Burki G., 1977, A&A 57, 135
Cousins A.W.J., 1978, Mon. Not. R. Astr. Soc. Sth. Afr. 37, 62
Conti P.S., 1988, in "O stars and Wolf-Rayet stars", Monograph Series of non-thermal phenomena in stellar atmospheres, CNRS and NASA, Conti P.S. and Underhill A. (eds.)
Crawford I.A., 1990, MNRAS 244, 646
Dame T.M., Ungerechts H., Cohens R.S., et al., 1987, ApJ 322, 706
Dean J.F., Warren P.R., Cousins A.W.J., 1978, MNRAS 183, 569
Eggen O.J., 1976, Q. Jl. R. Astr. Soc. 17, 472
Feinstein A., Ferrer O.E., 1968, PASP 80, 475
Garrison R.F., Schild R.E., 1979, AJ 84, 1020
Heske A., Wendker H.J., 1984, A&AS 57, 205
Heske A., Wendker H.J., 1985, A&A 151, 309
Hillenbrand L.A., Massey P., Strom S.E., Merrill K.M., 1993, AJ 106, 1906
Houck Th. E., 1956, Dissertation, University of Wisconsin.
Jerzykiewicz M., Pigulski A., Kopacki G., Mialkowska A., Niczyporuk S., 1996, Acta Astron. 46, 253
Johnson H.L., 1968, in Nebulae and Interstellar Matter, Middlehurst B.M. and Aller L.H. (eds.). The University of Chicago Press, p. 167
Kilian J., Montenbruck O., Nissen P.E., 1994, A&A 284, 437
Kholopov P.N., 1980, Soviet Astr. 24, 7
Laval A., 1972, A&A 19, 82
Levato H., Morrell N., 1983, ApJL 23, 183
Massa D., Fitzpatrick E.L., 1986, ApJS 60, 305
Massey P., Thompson A.B., 1991, AJ 101, 1408
Mermilliod J.-C., 1981, A&A 97, 235
Mihalas D., 1967, Galactic Astron. 4-5, p. 64
Neckel Th., Klare G., 1980, A&AS 42, 251
Perry C.L., Hill G., Younger P.F., Barnes J.V., 1990, A&AS 86, 415
Perry C.L., Hill G., Christodoulou D.M., 1991, A&AS 90, 195
Perry C.L., Hill G., 1992, A&A 257, 128
Piers R.P.A., The P.S., van Genderen A.M., 1992, A&AS 92, 609
Raboud D., 1996, A&A 315, 384
Raboud D., Cramer N., Bernasconi P.A., 1997, A&A 325, 167
Raboud D., 1998 (private communication)
Raboud D., Mermilliod J.-C., 1998, A&A 333, 897
Salpeter E.E., 1955, ApJ 121, 161
Santos J.F.C.jr, Bica E., 1993, MNRAS 260, 915
Scalo J., 1986, Fund. Cos. Phys. 11, 144
Schaller G., Schaerer D., Meynet G., Maeder A., 1992, A&AS 96, 269
Schmidt-Kaler Th., 1982, in Landolt-Bornstein VI/2b
Shapley H., 1930, Star Clusters, Harvard Obs. Mon., No. 2
Shobbrook R.R., 1983, MNRAS 205, 1229
Seggewiss W., 1968, Veroff. Astron. Inst. Bonn, No. 79
Stetson P.B., 1987, PASP 99, 191
Sung H., Bessell M.S., Lee S., 1998, AJ 115, 734
Trumpler R.J., 1930, Lick Obs. Bull. 14, 154
van Genderen A.M., Bijleveld W., van Groningen E., 1984, A&AS 58, 537
Underhill A., 1960, ApJ 131, 524
Vázquez R.A., Feinstein A., 1991, A&AS 90, 317
Vázquez R.A., Baume G., Feinstein A., Prado P., 1994, A&AS 106, 339
Vázquez R.A., Will J.-M., Prado P., Feinstein A., 1995, A&AS 111, 85
Vázquez R.A., Baume G., Feinstein A., Prado P., 1996, A&AS, 116, 75
Will J.-M., Vázquez R.A., Feinstein A., Seggewiss W., 1995, A&A 301, 396
Will J.-M., 1996, Inaugural-Dissertation zur Erlangung des Doktorgrades, Matematisch-Naturwissenschaftlichen Fakultat, Uni. Bonn